Projective-truncation-approximation study of the one-dimensional ϕ^4 lattice model

Kou-Han Ma, Yan-Jiang Guo, Lei Wang, and Ning-Hua Tong[*]

Department of Physics, Renmin University of China, 100872 Beijing, China

In this paper, we first develop the projective truncation approximation (PTA) in the Green's function equation of motion (EOM) formalism for classical statistical models. To implement PTA for a given Hamiltonian, we choose a set of basis variables and projectively truncate the hierarchical EOM. We apply PTA to the one-dimensional ϕ^4 lattice model. Phonon dispersion and static correlation functions are studied in detail. Using one- and two-dimensional bases, we obtain results identical to and beyond the quadratic variational approximation, respectively. In particular, we analyze the power-law temperature dependence of the static averages in the low- and high-temperature limits, and we give exact exponents.

I. INTRODUCTION

Classical many-body systems are an important research topic in condensed-matter physics, covering such diverse subjects as a state equation of atomic/molecular gases [1], glass formation in liquid [2], anomalous heat conductivity in low-dimensional atomic chains [3], a structural phase transition [4], etc. An accurate and efficient solution of the related classical statistical models plays a central role in the theoretical study. Modern computer-based techniques such as Monte Carlo and molecular dynamics are powerful but not sufficient to solve all the problems, due to their limitations from the computational complexity in size and time. Analytical methods, such as mode-coupling theory [5], the renormalization group [6], the variational method [7,8], etc., are still extensively used in the study. The present work is an effort to promote one of the analytical methods, namely the Green's function (GF) equation of motion (EOM), to an advanced level. We apply it to the study of a one-dimensional ϕ^4 lattice model for interacting particles on a chain. By enlarging the size of the variable basis, we obtain improved phonon dispersion and static averages, demonstrating the applicability of the proposed method to classical statistical models with continuous variables. Qualitatively accurate temperature dependence behavior in the low- and high-temperature limit can be extracted from our analysis.

The formalism of the EOM of a double time GF has a long history. It was developed first for quantum system in the 1950s [9–12] and then generalized to classical systems by Bogoliubov and Sadovnikov using a variational technique [13]. Herzel rederived the EOM of the classical GF [14] using the double time theory of Rostoker [15] and the Heisenberg picture for classical statistics [16]. A many-time GF and the resolvent formalism of the classical GF were subsequently developed by Herzel [17]. The meaning of these GFs as linear and higher-order response coefficients to external time-dependent perturbation was elaborated on in Refs. [18] and [19]. Applying this method to ideal gas, Smith obtained the exact density-density correlation function [20]. Campana *et al.* introduced the spectral function of the classical GF and proved the spectral theorem [21]. A closely related method, namely the spectral density method [22], was transplanted from quantum systems to classical systems and was applied to a variety of classical many-body statistical problems [21,23–25]. A Callen-type decoupling truncation of the hierarchical EOM was carried out for the classical Heisenberg model [26,27].

In the EOM method, a lower-order GF is related to a higher-order one and so on, until at some point this chain has to be truncated to form closed equations for GFs [28]. Traditional truncation procedures often rely heavily on physical intuition and are difficult to generalize. Certain analytical requirements of GFs, such as the sum rule, the positiveness of spectral weight, and real simple poles, are hard to guarantee by truncation approximations. In addition, the chain of the EOM will involve many averages, which are usually calculated self-consistently from the GFs via the fluctuation-dissipation theorem. Due to truncation, the number of unknowns could exceed the number of equations, and some additional approximations need to be invoked. All of these challenges make the traditional truncation approximation of the EOM a poorly controlled method.

Based on the idea of operator projection [29,30], a projective truncation approximation (PTA) was developed for quantum systems [31] to overcome the shortcomings of the traditional truncation approximation mentioned above. In this work, we adopt the same idea and develop a PTA for the classical statistical models. We apply the PTA to the study of the one-dimensional ϕ^4 lattice model [32,33], both to demonstrate the applicability of the method and to disclose the underlying physics of this model. This model has been the focus of a series of studies in the context of low-dimensional heat transport [32–39] and chaotic dynamics [40,41]. The existence of a quartic potential in this model opens a gap in the phonon spectrum at finite temperature and leads to normal heat trans-

[*]nhtong@ruc.edu.cn

port behavior. The phonon dispersion has been analyzed using various methods, such as the theories of self-consistent phonons (i.e., the quadratic variational method) [42], effective phonons [43], anharmonic phonons [44], and resonance phonons [38]. Among them, the first one is an analytical method and the latter three require numerical results as input.

In this study, we focus on the phonon dispersion and static averages of this model. To implement PTA, we need to choose a set of basis variables to projectively truncate the EOM. Using one- and two-dimensional bases within PTA, respectively, we obtain results identical to and beyond those from the variational method with a quadratic reference Hamiltonian, respectively. Our method provides a way to calculate the phonon spectrum of nonlinear lattice systems. The temperature dependence of static averages is also analyzed. We argue that the obtained asymptotic low- and high-temperature power laws are qualitatively exact.

The rest of this paper is arranged as follows. For completeness, we first review the formalism of the GF EOM for classical systems in Sec. II. In Sec. III, we develop the formalism of PTA for a classical system. In Sec. IV, we apply PTA to the one-dimensional ϕ^4 lattice model, and we summarize the formulas. Section V is devoted to a discussion of PTA results under different bases. A summary and discussion are given in Sec. VI.

II. DOUBLE-TIME GREEN'S FUNCTION EQUATION OF MOTION

In this section, we give a pedagogic review of the GF EOM for a classical system, setting up the framework for the PTA in the next section. A complete discussion can be found in Ref. [24]. Compared to the existing formalism of the EOM [14,24], in this work the fluctuation-dissipation theorem is modified such that it is applicable to variables with finite static components.

Suppose we have a classical system with canonical ordinates $(q_1, q_2, \ldots, q_N)$ and momenta $(p_1, p_2, \ldots, p_N)$. The Hamiltonian $H(q, p)$ describes a conserving system without dissipative forces. Here and below, we will use q and p as the short-hand notions for $(q_1, q_2, \ldots, q_N)$ and $(p_1, p_2, \ldots, p_N)$, respectively. In this paper, we only consider a Hamiltonian and dynamical variables that do not explicitly contain time t, such as $A(q, p)$ and $B(q, p)$. The time evolution of $q(t)$ and $p(t)$ is determined by Hamilton's equations,

$$\frac{dq_i(t)}{dt} = \frac{\partial H(q, p)}{\partial p_i}\Big|_{q=q(t),\, p=p(t)},$$
$$\frac{dp_i(t)}{dt} = -\frac{\partial H(q, p)}{\partial q_i}\Big|_{q=q(t),\, p=p(t)}. \quad (1)$$

The Poisson bracket between two variables A and B is defined as

$$\{A(q, p), B(q, p)\}$$
$$\equiv \sum_{i=1}^{N} \left[\frac{\partial A(q, p)}{\partial q_i} \frac{\partial B(q, p)}{\partial p_i} - \frac{\partial A(q, p)}{\partial p_i} \frac{\partial B(q, p)}{\partial q_i} \right]$$
$$= \frac{\partial A(q, p)}{\partial q} \frac{\partial B(q, p)}{\partial p} - \frac{\partial A(q, p)}{\partial p} \frac{\partial B(q, p)}{\partial q}. \quad (2)$$

In the following, as in the third line of Eq. (2), we will neglect the summation over i and abbreviate q_i and p_i by q and p. The standard Poisson brackets $\{q_i, p_j\} = \delta_{ij}$ and $\{q_i, q_j\} = \{p_i, p_j\} = 0$ are special cases of Eq. (2). It is noted that the Poisson bracket defined above is invariant under the canonical transformation [45]. That is,

$$\{A(q, p), B(q, p)\}$$
$$= \frac{\partial A(q, p)}{\partial Q} \frac{\partial B(q, p)}{\partial P} - \frac{\partial A(q, p)}{\partial P} \frac{\partial B(q, p)}{\partial Q}, \quad (3)$$

with $Q_i = Q_i(q, p)$, $P_i = P_i(q, p)$ being the canonical transformation.

In terms of the Poisson bracket, the time evolution of $A(t) = A[q(t), p(t)]$ obeys the EOM,

$$\frac{d}{dt} A[q(t), p(t)] = \{A(q, p), H(q, p)\}(t). \quad (4)$$

Under this equation the energy is conserved, $dH[q(t), p(t)]/dt = 0$. Since $A[q(t), p(t)]$ follows a deterministic equation (4), we have an alternative representation for it, namely $A[q(t), p(t)] = A[q(0), p(0); t]$. This change of representation is actually a transition from the Schrödinger picture, where the state $\Gamma(t) = (q(t), p(t))$ evolves with time and the operator $A(q, p)$ does not, to the Heisenberg picture, where the state stays at $\Gamma(0) = (q(0), p(0))$ while the operators evolve [16,18]. At $t = 0$, the two pictures coincide.

The retarded Green's function of two dynamical variables $A[q(t), p(t)]$ and $B[q(t'), p(t')]$ is defined as [14,20,23,24]

$$G^r[A(t)|B(t')] \equiv \theta(t - t')\langle\{A(t), B(t')\}\rangle. \quad (5)$$

Here $\theta(x)$ is the Heaviside step function. $\langle O \rangle$ is the average of variable O in an equilibrium state. $\{\cdots\}$ is the Poisson bracket defined in Eq. (2). Equation (5) gives the linear-response coefficient of $\langle A(t) \rangle$ under a weak perturbation proportional to $B(t')$[18,19]. Some remarks about the definition (5) are in order. For variables at unequal times $A(t)$ and $B(t')$, it is more convenient to use the Poisson bracket Eq. (3) and choose a special set of canonical variables, $Q_i(q, p) = q_i(0)$, $P_i(q, p) = p_i(0)$. $\{A(t), B(t')\}$ in Eq. (5) is then written in the Heisenberg picture as

$$\{A(t), B(t')\} = \frac{\partial A[q(0), p(0); t]}{\partial q(0)} \frac{\partial B[q(0), p(0); t']}{\partial p(0)}$$
$$- \frac{\partial A[q(0), p(0); t]}{\partial p(0)} \frac{\partial B[q(0), p(0); t']}{\partial q(0)}. \quad (6)$$

In addition to the usual properties of Poisson bracket, such as Jacobi's identity,

$$\{A(t_1), \{B(t_2), C(t_3)\}\} + \{B(t_2), \{C(t_3), A(t_1)\}\}$$
$$+ \{C(t_3), \{A(t_1), B(t_2)\}\} = 0, \quad (7)$$

Eq. (6) also has the following notable properties:

$$\frac{\partial}{\partial t} \{A(t), B(t')\} = \left\{ \frac{\partial}{\partial t} A(t), B(t') \right\}, \quad (8)$$

and the cyclic relation

$$\int dq \int dp A(t_1)\{B(t_2), C(t_3)\}$$
$$= \int dq \int dp B(t_2)\{C(t_3), A(t_1)\}. \quad (9)$$

Equation (9) can be obtained from integrating by parts and neglecting the boundary term. It is valid when one of the operators among $A(t_1)$, $B(t_2)$, and $C(t_3)$ becomes zero at the boundary of the phase space. In particular, it holds when $A(t_1) = e^{-\beta H(q,p)}/Z$ is the equilibrium density operator.

In Gibbs statistical theory, a state of the studied system is described by the probability density $\rho(q, p, t)$ of the ensemble distribution. The time evolution of $\rho(q, p, t)$ is governed by the Liouville equation

$$\frac{d}{dt}\rho[q(t), p(t), t] = 0. \quad (10)$$

In the Schrödinger picture, the ensemble average of a physical quantity $O(q, p)$ is given as

$$\langle O \rangle(t) \equiv \int dq \int dp\, O(q, p)\rho(q, p, t). \quad (11)$$

Using the invariance of the phase-space volume $dq(0)dp(0) = dq(t)dp(t)$ and the Liouville theorem $d\rho[q(t), p(t), t]/dt = 0$, we obtain the expression in the Heisenberg picture,

$$\langle O \rangle(t) = \int dq(0) \int dp(0)O[q(0), p(0); t]\rho[q(0), p(0), 0]. \quad (12)$$

Equation (12) says that the ensemble average of $O(t)$ can be calculated by averaging $O[q(0), p(0), t]$ over the initial distribution of $q(0)$ and $p(0)$. This formalism is used in the definition of the Green's function in Eq. (5), with the equilibrium state $\rho(q, p, t)$ (considering a canonical ensemble here)

$$\rho(q, p, t) = \frac{1}{Z}e^{-\beta H(q,p)}. \quad (13)$$

The partition function is $Z = \int dq \int dp \exp[-\beta H(q, p)]$. Here and below, we neglect the factor $1/(N!h^N)$ for brevity. $\beta = 1/(kT)$ is the inverse temperature. It is easy to prove the time-translation invariance of equilibrium state averages, $\langle O(t) \rangle = \langle O \rangle$, $\langle A(t)B(t') \rangle = \langle A(t - \tau)B(t' - \tau) \rangle$, and $\langle \{A(t), B(t')\} \rangle = \langle \{A(t - \tau), B(t' - \tau)\} \rangle$. Taking the derivative of t on both sides of $\langle O(t) \rangle = \langle O \rangle$, we obtain an important conservation relation for arbitrary operator $O(q, p)$,

$$\langle \{O(q, p), H(q, p)\} \rangle = 0. \quad (14)$$

This equation has the virial identity $\langle \mathbf{\nabla} \cdot \vec{f}(q) \rangle = \beta \langle \vec{f}(q) \cdot \mathbf{\nabla} H \rangle$ as a special case [46]. Here, $\vec{f}(q)$ is a polynomial function of q. Letting $O(q, p) = q_i p_i$, we also obtain the generalized equipartition theorem $\langle q_i \partial H/\partial q_i \rangle = T$. It will be used to simplify the EOM and to analyze the properties of physical quantities in the low- and high-temperature limits for the one-dimensional ϕ^4 lattice model. The cyclic relation

Eq. (9) implies

$$\langle \{A(t), B(t')\} \rangle = \beta \langle \{A, H\}(t)B(t') \rangle$$
$$= -\beta \langle A(t)\{B, H\}(t') \rangle. \quad (15)$$

Let us now derive the EOM for $G^r[A(t)|B(t')]$. We do the derivative with respect to t on both sides of Eq. (5) and employ Eqs. (4) and (8). Note that in the Heisenberg picture where $A[q(t), p(t)] = A[q(0), p(0); t]$, we have $\partial A(t)/\partial t = dA(t)/dt$. We obtain

$$\frac{\partial}{\partial t}G^r[A(t)|B(t')] = \delta(t - t')\langle \{A, B\} \rangle + G^r[\{A, H\}(t)|B(t')].$$
$$(16)$$

The Fourier transformation of the GF is defined as

$$G^r(A|B)_\omega = \int_{-\infty}^{\infty} G^r[A(t)|B(t')]e^{i(t-t')(\omega+i\eta)}d(t - t'). \quad (17)$$

η is an infinitesimal positive number, and $G^r(A|B)_\omega$ is a function of $\omega + i\eta$. Combining Eqs. (16) and (17), we obtain the EOM for the retarded GF in the frequency domain,

$$(\omega + i\eta)G^r(A|B)_\omega = i\langle \{A, B\} \rangle + iG^r(\{A, H\}|B)_\omega. \quad (18)$$

This equation is usually expressed in a more compact form, i.e., the EOM of the Zubarev GF $G(A|B)_\omega$ [without the superscript r, obtained by substituting the argument $\omega + i\eta$ of $G^r(A|B)_\omega$ by ω] [12]. It reads

$$\omega G(A|B)_\omega = i\langle \{A, B\} \rangle + iG(\{A, H\}|B)_\omega. \quad (19)$$

The retarded GF $G^r(A|B)_\omega$ can be recovered by an analytical continuation of the Zubarev GF $G(A|B)_\omega$, i.e., $G^r(A|B)_\omega = G(A|B)_{\omega \to \omega + i\eta}$. Similarly, the derivative of Eq. (5) with respect to t' gives the right-hand side EOM,

$$\omega G(A|B)_\omega = i\langle \{A, B\} \rangle - iG(A|\{B, H\})_\omega. \quad (20)$$

The static averages of the equilibrium state can be obtained from the corresponding GF via the fluctuation-dissipation theorem [14,24]

$$\langle AB \rangle = \frac{1}{\beta} \int_{-\infty}^{\infty} \frac{\Lambda_{A,B}(\omega)}{\omega} d\omega + \langle A_0 B_0 \rangle. \quad (21)$$

Here, A_0 and B_0 are the zero-frequency components of $A(t)$ and $B(t)$, respectively. The precise definition and some properties of the zero-frequency component X_0 of a general variable X are summarized in Appendix B. The spectral function $\Lambda_{A,B}(\omega)$ in the above equation is defined as [14,24]

$$\Lambda_{A,B}(\omega) \equiv \frac{i}{2\pi}[G(A|B)_{\omega+i\eta} - G(A|B)_{\omega-i\eta}]. \quad (22)$$

The proof of Eq. (21) is given in Appendixes A and B.

Note that in addition to a factor 2π difference in the definition, Eq. (21) is different from previous works [14,24] in that the contributions from static components of $A(t)$ and $B(t)$ are singled out. This equation has a wider application range than those in Refs. [14] and [24]. In the case in which A_0 or B_0 is a constant number, $\langle A_0 B_0 \rangle = \langle A \rangle \langle B \rangle$. In general, A_0 and B_0 are conserving quantities with possibly nonzero statistical fluctuations, and computing $\langle A_0 B_0 \rangle$ is a nontrivial task. This problem also arises in the commutator GF EOM formalism for quantum systems. Possible solutions are discussed in the

literature [47–50]. Similar methods can be used here to compute $\langle A_0 B_0 \rangle$ in the classical GF EOM formalism. For the ϕ^4 lattice model that we will study in this paper, $\langle A_0 B_0 \rangle = 0$ (see below).

III. PROJECTIVE TRUNCATION APPROXIMATION

The above formalism of the GF EOM is standard and has been obtained in previous works. In this section, we present the noteworthy development of this work, i.e., introducing PTA into the GF EOM for classical systems. PTA was proposed by Fan *et al.* first for the quantum GF EOM [31]. It is a systematic method for truncating the EOM, and it has controllable precision [51]. Recently, this method was used in the study of a phase diagram of a two-dimensional spinless fermion model [52]. Given the similar structure of the EOM in quantum and classical cases, PTA can well be transplanted to the classical GF EOM, with the special structure of a classical system taken into account.

We first generalize the GF EOM formalism to matrix form. Suppose we have a vector of basis variables $\vec{A} = (A_1, A_2, \ldots, A_n)^T$ that are in general complex. We assume a real Hamiltonian H and that the coordinates q_i and momenta p_i can be canonically transformed into real variables. Due to the invariance of the Poisson bracket under a canonical transformation of variables, the formula in the previous section still applies to complex variables $\{A_i\}$. We have $\langle O \rangle^* = \langle O^* \rangle$ and $\{X(t), Y(t')\}^* = \{X^*(t), Y^*(t')\}$.

The matrix of the retarded GF is defined as

$$G^r(\vec{A}(t)|\vec{A}^\dagger(t')) \equiv \theta(t - t')\langle\{\vec{A}(t), \vec{A}^\dagger(t')\}\rangle. \quad (23)$$

The Fourier transformation of the GF and the spectral density function are given, respectively, as

$$G^r(\vec{A}|\vec{A}^\dagger)_\omega = \int_{-\infty}^{\infty} d(t - t')G^r[\vec{A}(t)|\vec{A}^\dagger(t')]e^{i(\omega + i\eta)(t - t')} \quad (24)$$

and

$$\Lambda_{\vec{A}, \vec{A}^\dagger}(\omega) = \frac{i}{2\pi}[G(\vec{A}|\vec{A}^\dagger)_{\omega + i\eta} - G(\vec{A}|\vec{A}^\dagger)_{\omega - i\eta}]. \quad (25)$$

The fluctuation-dissipation theorem is generalized into

$$\mathbf{C} = \frac{1}{\beta} \int_{-\infty}^{\infty} d\omega \frac{\Lambda_{\vec{A}, \vec{A}^\dagger}(\omega)}{\omega} + \mathbf{C}_0. \quad (26)$$

Here, the correlation matrix $\mathbf{C}_{n \times n}$ has the element $\mathbf{C}_{ij} = \langle A_i^* A_j \rangle$. $(\mathbf{C}_0)_{ij} = \langle A_{i0}^* A_{j0} \rangle$ is the correlation of zero-frequency components A_{i0} and A_{j0} of the basis variables A_i and A_j. $\mathbf{C}$ and $\mathbf{C}_0$ are both Hermitian and positive-definite matrices. The two EOMs of the GF matrix read

$$\omega G(\vec{A}|\vec{A}^\dagger)_\omega = i\langle\{\vec{A}, \vec{A}^\dagger\}\rangle + iG(\{\vec{A}, H\}|\vec{A}^\dagger)_\omega \quad (27)$$

and

$$\omega G(\vec{A}|\vec{A}^\dagger)_\omega = i\langle\{\vec{A}, \vec{A}^\dagger\}\rangle - iG(\vec{A}|\{\vec{A}^\dagger, H\})_\omega. \quad (28)$$

Before making PTA, we first invoke a special feature of the classical dynamics. It has been observed that the classical GF always has poles in plus-and-minus pairs [24,53]. This reminds us that there could be some structure in the Poisson brackets between the basis variables and H. We can

classify all the dynamical variables into two categories: $\{O\} = \{O_e\} \cup \{O_o\}$. They satisfy $\langle\{O_e, O_e'\}\rangle = 0$ and $\langle\{O_o, O_o'\}\rangle = 0$. A natural classification strategy that fulfills this requirement is

$$\{O_e\} = \left\{ f(q) \prod_i p_i^{m_i} \,\middle|\, \sum_i m_i = 2k, \ k \in \mathbb{Z} \right\},$$

$$\{O_o\} = \left\{ g(q) \prod_i p_i^{n_i} \,\middle|\, \sum_i n_i = 2k + 1, \ k \in \mathbb{Z} \right\}. \quad (29)$$

$f(q)$ and $g(q)$ are arbitrary functions of q. If H has the form $H = \sum_i p_i^2/(2\mu_i) + V(q)$, it is easy to prove that $\{\{O_e, H\}, H\} \in \{O_e\}$ and $\{\{O_o, H\}, H\} \in \{O_o\}$. That is, a basis inside $\{O_e\}$ or $\{O_o\}$ will remain so after being acted on twice by $\{\ldots, H\}$. We therefore consider to iterate the EOM twice and truncate the high-order variable $\{\{\vec{A}, H\}, H\}$. Choosing the basis operators $\{A_i\}$ from one of the subspaces, we have $\langle\{\vec{A}, \vec{A}^\dagger\}\rangle = 0$. The second-order EOMs in matrix form are then obtained as

$$\omega^2 G(\vec{A}|\vec{A}^\dagger)_\omega = -\langle\{\{\vec{A}, H\}, \vec{A}^\dagger\}\rangle - G(\{\{\vec{A}, H\}, H\}|\vec{A}^\dagger)_\omega \quad (30)$$

and

$$\omega^2 G(\vec{A}|\vec{A}^\dagger)_\omega = \langle\{\vec{A}, \{\vec{A}^\dagger, H\}\}\rangle - G(\vec{A}|\{\{\vec{A}^\dagger, H\}, H\})_\omega. \quad (31)$$

To make PTA, we define the inner product of two variables A and B as

$$(A|B) \equiv \langle\{A^*, \{B, H\}\}\rangle. \quad (32)$$

Considering that $\{\{\vec{A}, H\}, H\}$ contains only a nonzero-frequency component (see Appendix B), we approximate it as

$$\{\{\vec{A}, H\}, H\} \approx -\mathbf{M}^T \bar{\vec{A}}, \quad (33)$$

where $\bar{A}_i \equiv A_i - A_{i0}$ is the nonzero-frequency component of A_i. This approximation is an extension of the Tyablikov-type decoupling approximation [11] $G(OA|B)_\omega \approx \langle O \rangle G(A|B)_\omega$ to the multicomponent case. It decouples the hierarchical EOMs into closed linear equations of GFs that are easy to solve. In the present work, as for the quantum systems [31], we determine the expansion coefficients $\mathbf{M}$ by projection. Projecting Eq. (33) to A_k and using the properties of static component A_{i0} listed in Appendix B, we obtain $\mathbf{M} = \mathbf{I}^{-1}\mathbf{L}$. Here, the Liouville matrix $\mathbf{L}$ is defined as

$$L_{ij} = -(A_i|\{\{A_j, H\}, H\}). \quad (34)$$

$\mathbf{I}$ is the inner product matrix with elements $\mathbf{I}_{ij} = (A_i|A_j)$. Using Eqs. (7) and (15), we find $I_{ij} = \beta\langle\{A_i^*, H\}\{A_j, H\}\rangle$ and $L_{ij} = \beta\langle\{\{A_i^*, H\}, H\}\{\{A_j, H\}, H\}\rangle$. Both $\mathbf{I}$ and $\mathbf{L}$ are thus positive-semidefinite Hermitian matrices. $\mathbf{M}$ is then guaranteed to have real positive eigenvalues.

The above method for determining $\mathbf{M}$ in Eq. (33) has several advantages over the traditional decoupling methods [11]. It gives the best linear approximation of $\{\{\vec{A}, H\}, H\}$ in the subspace $\{A_i\}$ in the sense that the distance between $\{\{\vec{A}, H\}, H\}$ and $-\mathbf{M}^T \bar{\vec{A}}$ (defined with respect to the given inner product) is the minimum one among all choices of $\mathbf{M}$.

It fulfills the physical requirements that a GF has only real simple poles and that $G(A_i|A_i)_\omega$ has positive weights in the $\omega > 0$ regime. When the basis $\{A_i\}$ is complete, or it contains a certain subspace of eigenmodes of H, this approximation becomes exact. So we expect that PTA is a good approximation when the coordinates of the eigenmodes of H are adequately expressed by the linear combination of basis variables. Studies show that as the basis is enlarged, the approximation is improved systematically [57].

Substituting Eq. (33) into Eq. (30), an approximate solution of the GF matrix is obtained as

$$G(\vec{A}|\vec{A}^\dagger)_\omega \approx (\omega^2 - \mathbf{M}^T)^{-1}\mathbf{I}^T, \tag{35}$$

or in terms of $\mathbf{U}$ and $\mathbf{\Lambda}$,

$$G(\vec{A}|\vec{A}^\dagger)_\omega \approx (\mathbf{IU})^*(\omega^2\mathbf{1} - \mathbf{\Lambda})^{-1}(\mathbf{IU})^T. \tag{36}$$

Here, $\mathbf{U}$ is the eigenvector matrix of $\mathbf{M}$, and $\mathbf{\Lambda} = \text{diag}(\lambda_1, \lambda_2, \dots, \lambda_n)$ is the eigenvalue matrix, with λ_k being real and $\lambda_k \geqslant 0$ for all k. They can be obtained by solving the generalized eigenvalue problem,

$$\mathbf{LU} = \mathbf{IU\Lambda}. \tag{37}$$

$\mathbf{U}$ satisfies the generalized unitary condition $\mathbf{U}^\dagger\mathbf{IU} = \mathbf{1}$. The element of the GF matrix reads

$$G(A_i|A_j^*)_\omega \approx \sum_k \frac{(\mathbf{IU})_{ik}^*(\mathbf{IU})_{jk}}{\omega^2 - \lambda_k}. \tag{38}$$

The fluctuation-dissipation theorem Eq. (26) produces the following equations for the averages:

$$\langle A_j^* A_i \rangle \approx \sum_k \frac{(\mathbf{IU})_{ik}^*(\mathbf{IU})_{jk}}{\beta\lambda_k} + \langle A_{j0}^* A_{i0} \rangle. \tag{39}$$

An equivalent expression is

$$\mathbf{C} \approx \frac{1}{\beta}\mathbf{IL}^{-1}\mathbf{I} + \mathbf{C}_0, \tag{40}$$

which does not require the solution of a generalized eigenvalue problem. Here, $\mathbf{C}$ and $\mathbf{C}_0$ are the correlation matrices defined below Eq. (26).

Similarly, we can derive expressions for the GF $G(\vec{A}|O^*)_\omega$ for arbitrary variable O as

$$G(\vec{A}|O^*)_\omega \approx (\omega^2\mathbf{1} - \mathbf{M}^T)^{-1}(O|\vec{A})$$
$$= (\mathbf{IU})^*(\omega^2\mathbf{1} - \mathbf{\Lambda})^{-1}\mathbf{U}^T(O|\vec{A}). \tag{41}$$

The averages are given as

$$\langle O^* A_i \rangle \approx \sum_{k,p} \frac{(\mathbf{IU})_{ik}^*\mathbf{U}_{pk}(O|A_p)}{\beta\lambda_k} + \langle O_0^* A_{i0} \rangle, \tag{42}$$

or in vector form,

$$\langle O^*\vec{A}^T \rangle \approx \frac{1}{\beta}(O|\vec{A}^T)\mathbf{L}^{-1}\mathbf{I} + \langle O_0^*\vec{A}_0^T \rangle. \tag{43}$$

If the matrices $\mathbf{L}$ and $\mathbf{I}$ are expressible by $\mathbf{C}$, i.e., $\mathbf{L} = \mathbf{L}(\mathbf{C})$ and $\mathbf{I} = \mathbf{I}(\mathbf{C})$, and if $\mathbf{C}_0$ can be calculated, Eq. (39) [or Eq. (40)] closes the equation for $\mathbf{C}$. Solving this equation can provide approximate values for the static correlation functions. The GF is then obtained from Eq. (35). If $\mathbf{L}$ and $\mathbf{I}$ involve the averages other than elements of $\mathbf{C}$, one needs to

resort to Eq. (43) for additional equations. The conservation relation Eq. (14) could also provide additional constraints on the involved averages. The whole scheme is similar to the quantum case [31].

IV. THE ONE-DIMENSIONAL NONLINEAR ϕ^4 LATTICE

In this section, we apply PTA to the classical one-dimensional ϕ^4 lattice model with the following Hamiltonian:

$$H = \sum_{i=1}^L \left[\frac{p_i^2}{2m} + V(x_i - x_{i-1}) + U(x_i) \right], \tag{44}$$

with

$$V(x_i - x_{i-1}) = \frac{K}{2}(x_i - x_{i-1})^2,$$
$$U(x_i) = \frac{\gamma}{4}x_i^4. \tag{45}$$

Here, L is the total number of classical particles. x_i represents the deviation of the ith particle from its equilibrium position. The position of the ith particle is $q_i = ia + x_i$. K is the nearest-neighbor coupling strength, and γ is the coefficient of the on-site potential. Here, we use a periodic boundary condition and set the lattice constant $a = 1$ and mass $m = 1$. This model can be obtained by discretizing the classical ϕ^4 field theory [32,54]. It describes a harmonic-coupled chain of particles, with each particle in a local quartic potential well.

To employ the translational symmetry of H, we express Eq. (44) in wave-vector space as

$$H = \sum_k H_k,$$
$$H_k = \frac{P_k P_k^*}{2} + \frac{\omega_0(k)^2}{2}Q_k Q_k^* + \frac{\gamma}{4}Q_k R_k^*. \tag{46}$$

Here, $\omega_0(k)^2 = 2K[1 - \cos(k)]$, $Q_k = 1/\sqrt{L}\sum_j e^{-ijk}x_j$, and $R_k = 1/\sqrt{L}\sum_j e^{-ijk}x_j^3$. The conjugate momentum of Q_k is $P_k = 1/\sqrt{L}\sum_j e^{ijk}p_j$. They satisfy the relation $\{Q_k, P_{k'}\} = \delta_{k,k'}$.

Similar to the Fermi-Pasta-Ulam (FPU)-β model [55], this ϕ^4 lattice model has an interesting scaling property [32]. Using the scaling transformation

$$p_i = \frac{K}{\sqrt{\gamma}}\tilde{p}_i, \quad x_i = \sqrt{\frac{K}{\gamma}}\tilde{x}_i, \tag{47}$$

one obtains

$$H = \frac{K^2}{\gamma}\widetilde{H}, \tag{48}$$

where the dimensionless Hamiltonian $\widetilde{H}$ reads

$$\widetilde{H} = \sum_{i=1}^L \left[\frac{\tilde{p}_i^2}{2} + \frac{1}{2}(\tilde{x}_i - \tilde{x}_{i-1})^2 + \frac{1}{4}\tilde{x}_i^4 \right]. \tag{49}$$

This implies a scaling form of physical quantities. For example,

$$\langle x_i^2 \rangle(K, \gamma, T) = \frac{K}{\gamma} \langle x_i^2 \rangle \left(1, 1, \frac{\gamma T}{K^2}\right),$$

$$\langle x_i^4 \rangle(K, \gamma, T) = \frac{K^2}{\gamma^2} \langle x_i^4 \rangle \left(1, 1, \frac{\gamma T}{K^2}\right),$$

$$C_v(K, \gamma, T) = C_v \left(1, 1, \frac{\gamma T}{K^2}\right),$$

$$\xi(K, \gamma, T)) = \xi \left(1, 1, \frac{\gamma T}{K^2}\right). \tag{50}$$

Here, $C_v = (1/L)\partial\langle H\rangle/\partial T$ is the isovolumetric specific-heat capacity and ξ is the correlation length defined as $\langle x_i x_j \rangle \sim e^{-|i-j|/\xi}$, $|i - j| \to \infty$.

Similar scaling relations exist for GFs. By moment expansion of GF, we obtain

$$G(x^m p^n | x^r p^s)(K, \gamma, T, \omega)$$
$$= K^{\theta_K} \gamma^{\theta_\gamma} G(x^m p^n | x^r p^s) \left(1, 1, \frac{\gamma T}{K^2}, \frac{\omega}{\sqrt{K}}\right), \tag{51}$$

with the scaling exponents $\theta_K = (m + r)/2 + n + s - 2$ and $\theta_\gamma = -(m + r + n + s)/2 + 1$. In the above equation, x^m is the short-hand notation for $x_1^{m_1} x_2^{m_2} \cdots x_L^{m_L}$ with $m_1 + m_2 + \cdots + m_L = m$. p^n is a similar notation. Taking $m = r = 1$ and $n = s = 0$, we obtain

$$G(Q_k | Q_k^*)(K, \gamma, T, \omega) = \frac{1}{K} G(Q_k | Q_k^*) \left(1, 1, \frac{\gamma T}{K^2}, \frac{\omega}{\sqrt{K}}\right). \tag{52}$$

Using the spectral decomposition of the classical GF [24] $G(\omega) = \sum_k W_k/(\omega - E_k)$ and assuming that poles E_k and weights W_k scale independently, we find the following scaling relations:

$$E_k(K, \gamma, T) = \sqrt{K} E_k \left(1, 1, \frac{\gamma T}{K^2}\right),$$

$$W_k(K, \gamma, T) = K^{\theta_K} \gamma^{\theta_\gamma} W_k \left(1, 1, \frac{\gamma T}{K^2}\right), \tag{53}$$

with $\theta_K = (m + r)/2 + n + s - 3/2$ and $\theta_\gamma = -(m + r + n + s)/2 + 1$. Here, we have allowed the quasiparticle energy E_k to be temperature-dependent. In particular, Eq. (53) implies that the phonon gap has the scaling relation $\Delta(K, \gamma, T) = \sqrt{K}\Delta(1, 1, \gamma T/K^2)$. Since the projection truncation of GFs conforms to the scaling transformation, we expect that PTA obeys all the above scaling relations. Indeed, with PTA numerical data, we numerically checked Eqs. (50), (52), and that for $\Delta(K, \gamma, T)$ and found perfect agreement.

Some exact relations about H can be obtained from the conservation relation Eq. (14). Taking $O = x_i^n p_i$ and $O = Q_k P_k$ in Eq. (14), respectively, we obtain

$$\gamma\langle x_i^{n+3}\rangle + 2K\langle x_i^{n+1}\rangle - K\left(\langle x_i^n x_{i-1}\rangle + \langle x_i^n x_{i+1}\rangle\right) = nT\langle x_i^{n-1}\rangle \tag{54}$$

and

$$\omega_0(k)^2\langle Q_k Q_k^*\rangle + \gamma\langle Q_k R_k^*\rangle = T. \tag{55}$$

Equation (54) with $n = 1$ and Eq. (55) are the generalized equipartition theorem (GET) in real space and wave-vector space, respectively. We have numerically checked that the PTA results, both from B1 and B2 bases (to be defined below), fulfill the above GET.

In the high-temperature limit, due to the large amplitude of oscillations, the x_i^4-term in H dominates the energy, and nonlocal correlation between particles can be ignored [39]. One expects that the system is well described by an independent anharmonic oscillator with Hamiltonian $H_s = p^2/2 + (\gamma/4)x^4$. It gives, in the limit $T \to \infty$,

$$\langle x^{2n} \rangle = 2^n \frac{\Gamma(\frac{n}{2} + \frac{1}{4})}{\Gamma(\frac{1}{4})} \gamma^{-\frac{n}{2}} T^{\frac{n}{2}}. \tag{56}$$

Here, $n = 0, 1, 2, \dots$. $\Gamma(1/4)$ and $\Gamma(n/2 + 1/4)$ are complete Γ functions. Through an integral of the equation of motion, the kinetic-temperature dependence of the frequency of this single oscillator is obtained exactly as

$$\omega_{\text{single}}(T) = \frac{\sqrt{2\pi}\Gamma(\frac{3}{4})3^{\frac{1}{4}}}{\Gamma(\frac{1}{4})} T^{\frac{1}{4}} \gamma^{\frac{1}{4}} \approx 1.115 T^{\frac{1}{4}} \gamma^{\frac{1}{4}}. \tag{57}$$

V. APPLYING PTA TO the ONE-DIMENSIONAL ϕ^4 LATTICE MODEL

A. Formalism

To apply PTA to the one-dimensional ϕ^4 lattice model Eq. (46), in this work we consider the following two bases: (i) basis B1: $\vec{A}_1 = (Q_k)^T$; and (ii) basis B2: $\vec{A}_2 = (Q_k, R_k)^T$. Q_k and R_k, as defined below Eq. (46), are Fourier transformations of x_i and x_i^3, respectively. Considering that the Hamiltonian is even under the two global parity transformations $x_i \to -x_i$ and $p_i \to -p_i$ ($i = 1, 2, \dots, L$), any conserved quantity $X(\{x_i, p_i\})$ should also be even, given that $\sum_i[\partial X/\partial x_i \partial H/\partial p_i] = \sum_i[\partial X/\partial p_i \partial H/\partial x_i]$. Since Q_k and R_k are odd under parity transformation, they do not have zero-frequency components, i.e., $Q_{k0} = R_{k0} = 0$. Therefore, we use $\mathbf{C}_0 = \mathbf{0}$ in Eqs. (26) and (40). As will be seen below, PTA under basis B1 gives identical results to self-consistent phonon theory (i.e., the quadratic variational method) [42]. PTA with basis B2 gives improved results over B1.

1. Basis B1: $\vec{A}_1 = (Q_k)^T$

For this one-dimensional basis, we obtain

$$I_{k,k'} = \delta_{k,k'},$$
$$L_{k,k'} = \omega(k)^2 \delta_{k,k'}. \tag{58}$$

Here, $\omega(k)^2 = \omega_0(k)^2 + (3\gamma)/L \sum_{k'}\langle Q_{k'}Q_{k'}^*\rangle$. Employing the spectral theorem and noting $Q_{k0} = 0$ for the ϕ^4 model, we get the self-consistent equation

$$\langle Q_k Q_k^* \rangle = \frac{1}{\beta\omega(k)^2}. \tag{59}$$

From the pole of $G(Q_k|Q_k^*)_\omega$, we obtain the phonon dispersion $\omega(k) = \sqrt{\omega_0(k)^2 + 3\gamma\langle x_i^2\rangle}$. It is the same as the result from self-consistent phonon theory (i.e., the quadratic variational method) [42]. In the PTA study of the spinless fermion model [52], the single anharmonic oscillator model [57], and

the FPU-β model, we found that under a one-dimensional single-particle basis, PTA results are identical to those from the variational method with a quadratic reference Hamiltonian. Though not yet proved rigorously, we believe that this is true in general. With an enlarged basis size, PTA within the GF EOM method could provide a convenient scheme for systematically going beyond the traditional variational approximation.

2. Basis B2: $\vec{A}_2 = (Q_k, R_k)^T$

For this two-dimensional basis, we obtain $\mathbf{I}_{kk'} = \mathbf{I}_k \delta_{k,k'}$, $\mathbf{L}_{kk'} = \mathbf{L}_k \delta_{k,k'}$, with

$$\mathbf{I}_k = \begin{pmatrix} 1 & 3f_1 \\ 3f_1 & 9f_2 \end{pmatrix} \tag{60}$$

and

$$\mathbf{L}_k = \begin{pmatrix} \omega(k)^2 & 3\omega_0(k)^2 f_1 + 9\gamma f_2 \\ 3\omega_0(k)^2 f_1 + 9\gamma f_2 & L_{22} \end{pmatrix}. \tag{61}$$

Here,

$$L_{22} = \frac{54}{\beta} f_1 + 54Kf_2 + 45\gamma f_3 - 36Kf_4 - 18K\cos(k)f_5. \tag{62}$$

The real functions f_1–f_5 are defined as

$$f_1 = \frac{1}{L}\sum_{k_1}\langle Q_{k_1}Q_{k_1}^*\rangle,$$

$$f_2 = \frac{1}{L}\sum_{k_1}\langle Q_{k_1}R_{k_1}^*\rangle,$$

$$f_3 = \frac{1}{L}\sum_{k_1}\langle R_{k_1}R_{k_1}^*\rangle,$$

$$f_4 = \frac{1}{L}\sum_{k_1}\cos(k_1)\langle Q_{k_1}R_{k_1}^*\rangle,$$

$$f_5 = \frac{1}{L}\sum_{k_1}e^{-ik_1}\langle Q_{k_1}^*O_{k_1}\rangle. \tag{63}$$

The variable O_k in f_5 in the above equation is defined as $O_k = (1/\sqrt{L})\sum_j e^{-ijk}x_j^2 x_{j+1}$. The average $\langle Q_{k_1}^*O_{k_1}\rangle$ needs to be calculated from the new GF $G(\vec{A}_2|O_k^*)_\omega$, following Eq. (41). The inner products used in this process are

$$(O_k|Q_k) = e^{-ik}f_1 + \frac{2}{L}\sum_{k_1}\cos(k_1)\langle Q_{k_1}Q_{k_1}^*\rangle,$$

$$(O_k|R_k) = 6f_4 + 3e^{-ik}f_5. \tag{64}$$

In the derivation of above equations, we have used the exact relation $\langle p^2\rangle = 1/\beta$. The positive-definiteness of $\mathbf{I}$ amounts to $\langle x^4\rangle - \langle x^2\rangle^2 > 0$, a physical requirement. The positive-definiteness of $\mathbf{L}$ also represents constraints on the averages.

B. Numerical results

Below, we present the numerical results obtained by solving the self-consistent equation (40) for the above two bases.
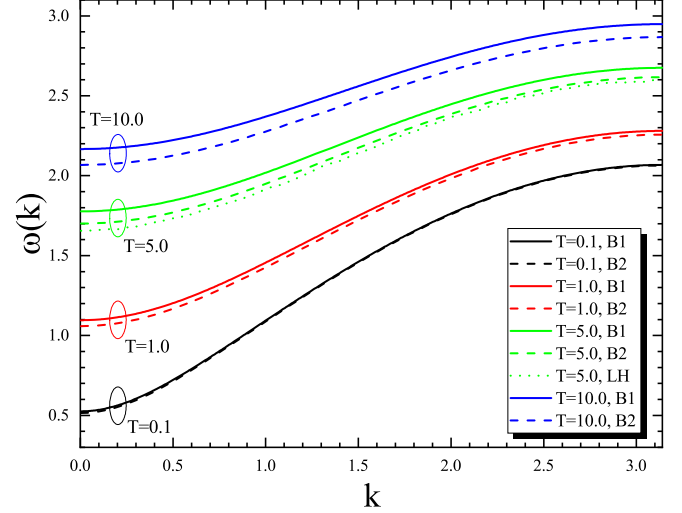

FIG. 1. Dispersion relation $\omega(k)$ at different temperatures. The solid and dashed lines are results from B1 and B2 bases, respectively. The green dotted line for $T = 5.0$ (LH) is from the lower bound harmonic variation of free energy obtained by Liu *et al.* [42].

Due to the scaling properties Eqs. (47)–(49), unless otherwise specified, we choose the model parameters $K = \gamma = 1$.

1. ϕ^4 lattice

Basis B1 produces a single excitation at $\omega(k)$. For basis B2, $G(Q_k|Q_k^*)_\omega$ has two poles on the positive frequency axis. One of them carries most of the weight. It is regarded as the phonon excitation. The other pole has only a tiny weight and is located at noninteger times of the phonon frequency. It is more like a satellite peak of the main peak rather than the overtone or combination tone frequently observed in the molecular/crystal vibrational spectrum. This satellite peak is dependent on the arbitrary choice of the basis not being a physical effect but rather a nondesired parasite. The appearance of a combination tone requires multiple fundamental frequencies, which is not the case for the monatomic ϕ^4 lattice model studied here. In classical system, anharmonicity makes the fundamental frequency energy-dependent and thus gives a broadened peak in the spectral function at finite T [56]. The overtone of the ϕ^4 lattice may manifest itself in the spectral function as a weak broad peak at integer times of the phonon frequency, similar to what we observed in molecular dynamics (MD) simulation of the power spectrum (not shown). It is expected to be obtained only in the large basis limit of PTA. Obtained from the two-dimensional basis B2, the pole with the tiny weight may well be a precursor of the broadening of the main peak. A detailed investigation of this issue using a larger basis will be the subject of a later study.

In Fig. 1, we show phonon dispersions obtained from B1 and B2 bases for a series of temperatures. For a given temperature, $\omega(k)$ is a monotonously increasing function with a gap at $k = 0$. B1 and B2 only produce quantitative differences. The difference approaches zero at low temperature (say $T = 0.1$) and enlarges with increasing temperature. This is expected since at low T, the anharmonic potential barely influences the small-amplitude oscillation of particles, and the
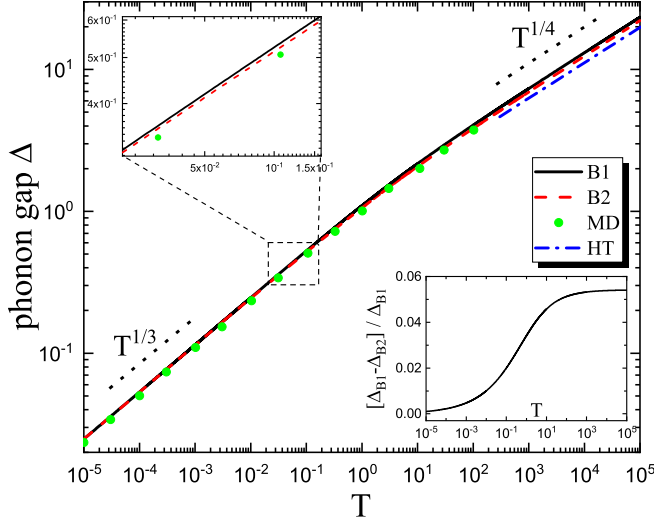
FIG. 2. Phonon gap as a function of temperature T. Green solid dots are from MD simulation. The blue dash-dotted line in the high-temperature regime (HT) is for Eq. (57). The black dotted lines are for guiding the eyes. Upper-left inset: enlarged part of the main figure. Lower-right inset: relative difference between B1 and B2 results.

FIG. 3. Correlation length ξ as a function of temperature T. The red dashed line marks the $T^{-1/3}$ power law.

quadratic variational approximation is adequate. At higher T, the anharmonic effect taken into account by B2 becomes more significant. For a given T, the B2 basis always produces lower $\omega(k)$ than B1 does, similar to the results of Ref. [42] where $\omega(k)$ from the lower bound harmonic variation lies below that from the upper bound variation. The former is expected to be more accurate since correlations are treated more adequately.

Note that the damping of the phonon excitation due to the x_i^4-term is not described within the B2 basis. As temperature increases, the phonon peak in the spectral function should be broadened significantly and finally smeared in the high-temperature limit (e.g., $T = 10$) where the phonon is no longer well defined [56]. In contrast, the B2 basis produces two δ-peaks in the spectral function at finite temperature. The quantitative improvement in the static quantities by the B2 basis therefore mainly comes from a better description of the spectral moments but not the damping. To describe the damping effect that is indispensable for the heat conductivity study, we need to either use a much larger basis dimension in PTA, or supplement PTA with a memory function calculation.

At finite temperature, a gap $\Delta(T)$ emerges in the phonon spectrum at $k = 0$ due to the existence of an on-site potential. This gap will significantly affect the heat transport behavior of the ϕ^4 model. Figure 2 compares $\Delta(T)$ obtained from various methods. B1 and B2 give qualitatively similar $\Delta(T)$. It has the low- and high-temperature asymptotic power laws as $\Delta(T) \sim T^{1/3}$ ($T \to 0$) and $\sim T^{1/4}$ ($T \to \infty$). The lower-right inset shows the relative error between B1 and B2 results. It increases from zero at $T = 0$ and saturates in the high-T limit.

The low-/high-temperature comparison of $\Delta(T)$ deserves separate discussions. In the high-temperature limit, the interparticle couplings are negligible and particles move basically independently. Then Eq. (57) gives the exact gap $\Delta(T)$ in the infinite-temperature limit and an upper bound of the gap at
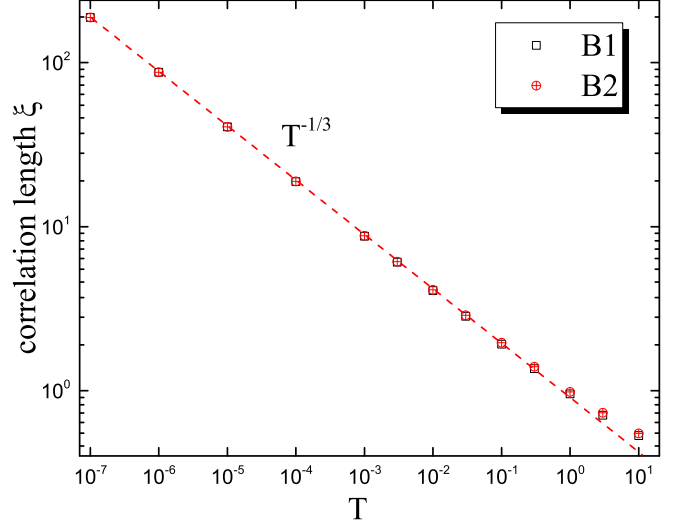
finite temperature. In Fig. 2, $\omega_{\mathrm{single}}(T)$ (see Eq. 57) is plotted as a blue dash-dotted line in the high-temperature regime. We see that both B1 and B2 are only slightly greater than $\omega_{\mathrm{single}}(T)$, and more importantly, B2 is in even better agreement.

In the low-temperature regime, $\langle x_i^2 \rangle \propto T^{2/3}$ [54], and thus the lattice can no longer be regarded as independent particles. Equation (57) does not apply. In such a case, in order to evaluate B1 and B2 we turn to calculating $\Delta(T)$ numerically using MD simulations. The simulations are carried out in a lattice with a periodic boundary condition and $L = 1000$ particles. A set of randomly chosen initial states are extracted from the microcanonical ensemble with fixed energy density $\langle E \rangle$, which corresponds to the desired temperature T. The power spectrum $S_k(\omega)$ of the mode with wave vector k, i.e., the Fourier transform of P_k [58], is then calculated after a long enough transient time. The profile of each power spectrum is basically a single peak. The frequency $\omega(k)$ can be simply determined by the location of the peak. The so-measured $\Delta \equiv \omega(0)$ as a function of T is plotted in Fig. 2 as well as in the upper-left inset as green circles. Again, we see that both B1 and B2 agree with the numerical simulation very well, and the agreement of B2 is even better. In summary, B1 and B2 bases give correct low- and high-temperature exponents of $\Delta(T)$. B2 gives quantitatively improved results over B1.

Figure 3 shows the temperature dependence of correlation length ξ, defined by $\langle x_i x_j \rangle \sim e^{-|i-j|/\xi}$ ($|i - j| \gg 1$). Both bases give $\xi \propto T^{-1/3}$ in the low-temperature limit. According to Eq. (50), the limit $T \to 0$ is equivalent to $\gamma \to 0$ or $K \to \infty$ for ξ. In this limit, the particles move along the chain with unbound but locked-in displacements $x_i = x_j$, giving $\xi = \infty$. Further, we find that the numerical results fulfill $\langle x_i x_j \rangle = \langle x_i^2 \rangle e^{-|i-j|/\xi}$ not only for large $|i - j|$ but also for short range. This helps us to understand the power exponent 1/3. Assigning $j = i + 1$ in the above equation, we have $\xi = 1/\ln[\langle x_i^2 \rangle / \langle x_i x_{i+1} \rangle]$. Employing the exact low-temperature asymptotic behaviors $\langle x_i^2 \rangle \approx \langle x_i x_{i+1} \rangle \propto T^{2/3}$ and $\langle x_i^2 \rangle - \langle x_i x_{i+1} \rangle \propto T$ (see Fig. 5 and its discussion), we obtain the relation $\xi \propto T^{-1/3}$. At high temperatures (say $T \sim 1$),
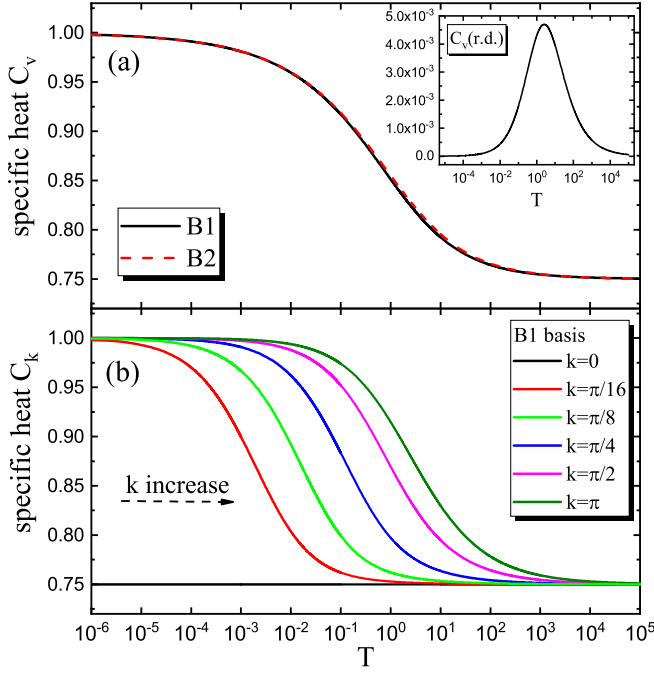
FIG. 4. Specific heat. (a) C_v and (b) C_k as functions of temperature T. Inset of (a): The relative difference between specific heat C_v from B1 and B2. $C_v(r.d.) = [C_v(B2) - C_v(B1)]/C_v(B1)$.

both B1 and B2 results deviate from $T^{-1/3}$ law, signaling that the system enters a strong chaotic regime [42,59,60].

Figure 4(a) shows the evolution of isovolumetric specific heat capacity C_v with temperature. Again, the results from
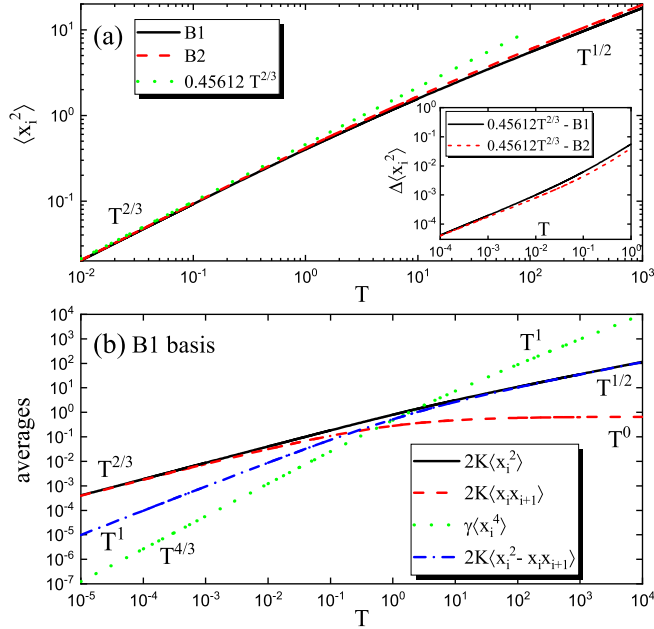

FIG. 5. Average of physical quantities as functions of T. (a) $\langle x_i^2 \rangle$ from the B1 and B2 bases are compared. The dotted line shows $0.456\,12T^{2/3}$ from the classical field method [54]. Inset: differences between PTA and classical field results. (b) B1 basis results for $2K\langle x_i^2 \rangle$, $2K\langle x_i x_{i+1} \rangle$, $\gamma\langle x_i^4 \rangle$, and $2K(\langle x_i^2 \rangle - \langle x_i x_{i+1} \rangle)$ as functions of T.

B1 and B2 bases have only a slight difference. With increasing temperature, C_v gradually decreases from $C_v = 1.0$ at $T = 0$ (equivalent to the harmonic limit) to 3/4 in the high-temperature limit. This behavior is similar to that of the FPU-β model [61]. It is not a coincidence, rather it is due to the thermodynamic similarity between the ϕ^4 model and the FPU-β model in the high- and low- temperature limits. By analysis of GET, we obtain $C_v = 1.0 - (\gamma/4)\partial\langle x_i^4 \rangle/\partial T$ and the low-/high-temperature asymptotic behaviors $\langle x_i^4 \rangle \ll T$ ($T \to 0$) and $\langle x_i^4 \rangle \approx T$ ($T \to \infty$). We thus confirm that the results of C_v in Fig. 4(a) are also exact in the high- and low- temperature limits. The crossover of C_v from low to high temperature occurs at around $T = 1.0$. As shown in the inset of Fig. 4(a), the relative difference between B1 and B2 turns out to be less than 0.5%, with the maximum near the crossover temperature.

Figure 4(b) presents the temperature dependence of single-mode specific heat C_k, defined as $C_k = \partial\langle H_k \rangle/\partial T$, and H_k defined in Eq. (46). Only the B1 result is shown here since the B2 result is quantitatively similar. $C_k(T)$ looks similar to $C_v(T)$, with a crossover temperature increasing with k. This is because the dispersion function $\omega(k)$ increases monotonously with k, as shown in Fig. 1. The excitation of a larger momentum phonon requires more energy, resulting in greater specific heat C_k. Similarly, the asymptotic high- and low-temperature limits of C_k are captured exactly by PTA. Note that $C_{k=0}(T) = 3/4$ for all T is an exact result, since the GET Eq. (55) gives $\gamma\langle Q_{k=0}R_{k=0}^* \rangle = T$ and $\langle H_{k=0} \rangle = 3T/4$.

Figure 5 shows the temperature dependence of several types of averages. We focus on $\langle x_i^2 \rangle$ in Fig. 5(a). It is found that $\langle x_i^2 \rangle \propto T^{2/3}$ ($T \to 0$) and $\langle x_i^2 \rangle \propto T^{1/2}$ ($T \to \infty$), with a crossover temperature around unity. Our result at low temperature agrees quantitatively with that from the classical field method [54] [dotted line in Fig. 5(a)]. In the high-temperature limit, $\langle x_i^2 \rangle \propto T^{1/2}$ can be understood from Eq. (56). Quantitatively, $\langle x_i^2 \rangle$ obtained by the B2 basis is slightly larger than that of the B1 basis. In the inset of Fig. 5(a), we compare the two PTA results with $\langle x_i^2 \rangle = 0.456\,12T^{2/3}$ of the classical field method. As expected, the B2 basis compares more favorably. We also studied $\langle x_i^2 \rangle$, $\langle x_i^4 \rangle$, $\langle x_i x_{i-1} \rangle$, etc., using MD. The MD results (not shown) agree very well with the B1 and B2 results.

For the ϕ^4 lattice model, Eq. (54) (with $n = 1$) gives the GET $\gamma\langle x_i^4 \rangle + 2K\langle x_i^2 \rangle - 2K\langle x_i x_{i+1} \rangle = T$. Figure 5(b) shows the temperature dependence of all averages appearing in this equation, obtained from the B1 basis. Our numerical results satisfy the GET within numerical error. All the curves in Fig. 5(b) have power-law behavior in the low- as well as high-temperature limits, with distinct powers and similar crossover temperatures around unity. This value of crossover temperature is comparable to the strong stochasticity threshold temperature of the ϕ^4 model [42,59,60].

Several noteworthy features of Fig. 5(b) are discussed in order. First, in $T \ll 1$, $\langle x_i^2 \rangle$ and $\langle x_i x_{i+1} \rangle$ have the same leading power, while in $T \gg 1$, $\langle x_i x_{i+1} \rangle \ll \langle x_i^2 \rangle$. This is consistent with the temperature-dependent behavior of the correlation length shown in Fig. 3, signaling the weakening of nonlocal correlation at high temperature. Second, in the low-temperature limit, $\langle x_i^2 \rangle \sim T^{2/3}$ and $\langle x_i^2 \rangle - \langle x_i x_{i+1} \rangle \sim T$, respectively. This is because when $T \to 0$ (equivalent to $\gamma \to 0$), the translational symmetry of the system gradually
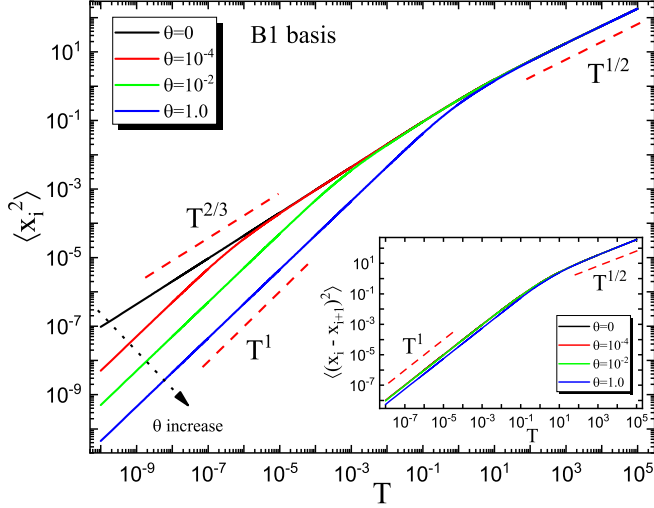
FIG. 6. $\langle x_i^2 \rangle$ as a function of T for the modified ϕ^4 model at various θ values. Inset: $\langle (x_i - x_{i+1})^2 \rangle$ as functions of T. The red dashed lines mark the corresponding power law.

recovers. The independent dynamic variable is not x_i but $x_{i+1} - x_i$. As a result, $\langle (x_{i+1} - x_i)^2 \rangle = 2(\langle x_i^2 \rangle - \langle x_i x_{i+1} \rangle) \propto T$ according to the equipartition theorem. Finally, for $\langle x_i^4 \rangle$, the variational approximation is considered to be reliable in $T \ll 1$. So $\langle x_i^4 \rangle \approx 3 \langle x_i^2 \rangle^2 \propto T^{4/3}$. In the high-temperature limit, GET guarantees $\langle x_i^4 \rangle \sim T$. In summary, the exact power exponents in the T-dependence of averages are obtained in Fig. 5.

2. Modified ϕ^4 lattice

In the low-temperature limit, $\langle x_i^2 \rangle \propto T^{2/3}$ is counterintuitive. To further understand the temperature dependence of $\langle x_i^2 \rangle$, we study a modified ϕ^4 model. Its Hamiltonian reads

$$H = \sum_{i=1}^{L} \left[\frac{p_i^2}{2m_i} + \frac{K}{2}(x_i - x_{i-1})^2 + \frac{\gamma}{4} x_i^4 + \frac{\theta}{2} x_i^2 \right]. \quad (65)$$

Here, a harmonic potential $(\theta/2)x_i^2$ is added. At $\theta = 0$, Eq. (65) recovers the standard ϕ^4 model. Historically, Eq. (65) with $\theta < 0$ (i.e., a double potential well) has been used to study the structural phase transition [62]. The breather mobility [63] and nonequilibrium statistical mechanical properties [64] of this model were studied. In this work, we focus on the single potential well case ($\theta \geqslant 0$), and we study the temperature dependence of $\langle x_i^2 \rangle$ and $\langle (x_i - x_{i+1})^2 \rangle$. As will be shown below, a nonzero harmonic potential will change the low-temperature behavior of $\langle x_i^2 \rangle$.

In Fig. 6, we show the temperature dependence of $\langle x_i^2 \rangle$ for several values of θ. In the high-temperature regime $T \gg T_{\text{high}}$, $\langle x_i^2 \rangle(T) \propto T^{1/2}$ and the coefficient is insensitive to θ. This is because the γ term dominates all the physical quantities in this limit. In the low-temperature regime $T \ll T_{\text{low}}$, a finite θ leads to a new asymptotic behavior $\langle x_i^2 \rangle \propto T$. In the intermediate temperature $T_{\text{low}} \ll T \ll T_{\text{high}}$, $\langle x_i^2 \rangle \propto T^{2/3}$. The two crossover temperatures T_{low} and T_{high} are controlled by θ and γ, respectively. We find that $T_{\text{low}} \sim \theta^{3/2}$ and $T_{\text{high}} \sim \gamma^{-1}$. In the limit $\theta = 0$, $T^{2/3}$ behavior extends to $T = 0$, recovering

the result of Fig. 5(a). For $\theta \approx 1.0$, $T_{\text{low}} \approx T_{\text{high}}$ and the intermediate $T^{2/3}$ regime disappears.

The inset of Fig. 6 shows $\langle (x_i - x_{i+1})^2 \rangle(T)$ for the same parameters. In contrast to $\langle x_i^2 \rangle$, $\langle (x_i - x_{i+1})^2 \rangle(T)$ does not change qualitatively with θ. At low temperature $T \ll T_{\text{high}}$, $\langle (x_i - x_{i+1})^2 \rangle \propto T$. At high temperature $T \gg T_{\text{high}}$, $\langle (x_i - x_{i+1})^2 \rangle \propto T^{1/2}$. Compared to $\langle x_i^2 \rangle$, $\langle (x_i - x_{i+1})^2 \rangle$ has only one crossover temperature T_{high}.

The rich physical behavior of Hamiltonian (65) is a result of a competition between $U_h(x)$ (harmonic potential), $U_{ah}(x)$ (anharmonic potential), $V(x)$ (nearest-neighbor harmonic coupling), and temperature T (kinetic energy). $U_h(x)$ dominates the shape of the bottom of the potential well, and $U_{ah}(x)$ dominates the regime away from the bottom and brings the correlation. At low temperatures, the small-amplitude oscillation of particles is mainly constrained by $U_h(x)$ and $V(x)$, leading to $\langle x_i^2 \rangle \propto T$ and $\langle (x_i - x_{i+1})^2 \rangle \propto T$, respectively. In the high-temperature limit, the large-amplitude and almost independent oscillations are dominated by $U_{ah}(x)$. So we have $\langle x_i^2 \rangle \sim \langle (x_i - x_{i+1})^2 \rangle \propto T^{1/2}$ according to Eq. (56). In the intermediate temperature region, the motion of the particles is jointly constrained by $U_h(x)$, $U_{ah}(x)$, and $V(x)$. The competition makes $\langle x_i^2 \rangle \propto T^{2/3}$, with the power index 2/3 lying between 1 [$U_h(x)$-dominant exponent] and 1/2 [$U_{ah}(x)$-dominant exponent].

VI. SUMMARY AND DISCUSSIONS

In this work, we developed PTA in the GF EOM formalism for classical systems. Using this method, we studied the one-dimensional ϕ^4 lattice model under two successively larger variable bases. The result from the one-dimensional B1 basis is found to be identical to that from the self-consistent phonon theory (equivalent to the quadratic variational method). The two-dimensional B2 basis gives quantitatively improved results. Qualitatively exact high- and low-temperature asymptotic behaviors for many static averages are obtained. The method presented in this work provides a way to calculate the phonon spectrum of nonlinear lattice systems.

Our results in this work show that PTA is a systematic method to go beyond the conventional variational method. There are many classical systems with interesting physical problems that would be challenging to study. One of them is the FPU model, which plays a central role in the study of the low-dimensional anomalous heat transport problem and phonon transistor design [65]. Another example is the molecular liquids, whose properties are very complicated and rich, especially close to the glass formation [66,67]. The Coulomb fluid is still another example, where ions carrying positive and/or negative charges are dispersed in a liquid. The Coulomb interactions among ions could induce a complicated phenomenon [68]. In all these fields, PTA within the GF EOM may be a useful tool.

The selection of basis is an important issue in PTA. In principle, we should incorporate in the basis those dynamical variables that are most relevant to the eigenmode of the system. In practice, there are different ways to systematically enlarge the basis. In this work, we start from the dynamical variable Q_k (B1 basis). We then add R_k, which is a variable appearing in the expression $\{\{Q_k, H\}, H\}$, to form the B2 basis.

We could collect the new variables appearing in $\{\{R_k, H\}, H\}$ to further enlarge the basis. There are other strategies, such as the Lanczos basis [69]. Different strategies of enlarging the basis could have different converging speeds. Finding an efficient basis selection strategy is an important issue to be studied in the future.

A related issue is the description of a spectral function by PTA. Further study [57] shows that while the static averages converge fast with increasing basis dimension, the spectral function depends more sensitively on the basis selection and converges slower. For classical systems, due to anharmonicity, the eigenmode frequencies depend on initial energy. Thermal averaging over initial states then broadens the excitation peaks at finite temperature, making them difficult to describe by a finite number of poles. As a result, for physical quantities for which the damping of quasiparticles or the broadening of a spectral function play a decisive role, such as a transport coefficient, the present method may be inefficient. To overcome this difficulty, one could also calculate the memory function [29,30] contribution to self-energy based on PTA, along the lines of Tserkovnikov [70]. The spectral density approximation [22] may be advantageous in this regard, which assumes a continuous spectral function from the outset. Preliminary results with a broadened spectral function have been obtained for the ϕ^4 lattice model and will be discussed elsewhere.

APPENDIX A: PROOF OF FLUCTUATION-DISSIPATION THEOREM

In this Appendix, we prove the fluctuation-dissipation theorem Eq. (21). The proof was originally given in Ref. [14]. Here we use a slightly different derivation.

The Fourier transformation of the GF, Eq. (17), reads

$$G^r(A|B)_\omega = \int_{-\infty}^{\infty} d(t-t')\theta(t-t')\langle\{A(t), B(t')\}\rangle e^{i(\omega+i\eta)(t-t')}.$$
(A1)

Now we define the two-time correlation function $F[A(t)|B(t')]$ as

$$F[A(t)|B(t')] = \langle A(t)B(t')\rangle.$$
(A2)

Its Fourier transformation $F(A|B)_\omega$ is given by

$$F(A|B)_\omega = \int_{-\infty}^{\infty} d(t-t')F[A(t)|B(t')]e^{i\omega(t-t')}.$$
(A3)

The EOM for $F[A(t)|B(t')]$ reads

$$\frac{\partial}{\partial t}F[A(t)|B(t')] = F[\{A, H\}(t)|B(t')].$$
(A4)

The Fourier transformation gives

$$\omega F(A|B)_\omega = iF(\{A, H\}|B)_\omega.$$
(A5)

It can be used to solve $F(A|B)_\omega$ except at $\omega = 0$. For example, for a constant variable $A = \alpha$, we have $\{A, H\} = 0$ and the EOM reads

$$\omega F(\alpha|B)_\omega = 0.$$
(A6)

It cannot be used to give the exact solution

$$F(\alpha|B)_\omega = 2\pi\alpha\langle B\rangle\delta(\omega).$$
(A7)

Using Eq. (15) obtained from the cyclic relation and the definition of $F[A(t)|B(t')]$, Eq. (A1) becomes

$$G^r(A|B)_\omega = \beta\int_0^{\infty} d(t-t')\left[\frac{\partial}{\partial t}F[A(t)|B(t')]\right]e^{i(\omega+i\eta)(t-t')}.$$
(A8)

We then obtain

$$G^r(A|B)_\omega = \frac{\beta}{2\pi}\int_{-\infty}^{\infty} d\omega'\frac{\omega'F(A|B)_{\omega'}}{\omega+i\eta-\omega'}.$$
(A9)

The corresponding Zubarev GF $G(A|B)_\omega$ reads

$$G(A|B)_\omega = \frac{\beta}{2\pi}\int_{-\infty}^{\infty} d\omega'\frac{\omega'F(A|B)_{\omega'}}{\omega-\omega'}.$$
(A10)

The spectral function $\Lambda_{A,B}(\omega)$ defined by Eq. (22) is obtained as

$$\Lambda_{A,B}(\omega) = \frac{\beta}{2\pi}\omega F(A|B)_\omega.$$
(A11)

Its Fourier transformation is

$$\Lambda_{A,B}(t-t') = \frac{i}{2\pi}\langle\{A(t)B(t')\}\rangle.$$
(A12)

At $t = t'$, it gives the sum rule

$$\int_{-\infty}^{\infty} d\omega\Lambda_{A,B}(\omega) = i\langle\{A, B\}\rangle.$$
(A13)

Further, from Eq. (A11), one can obtain $F(A|B)_\omega$ as

$$F(A|B)_\omega = \frac{2\pi}{\beta}\frac{\Lambda_{A,B}(\omega)}{\omega} + C_{A,B}\delta(\omega).$$
(A14)

$C_{A,B}$ is the contribution from zero-frequency components of $A(t)$ and $B(t')$. It is given by

$$C_{A,B} = 2\pi\langle A_0 B_0\rangle.$$
(A15)

Equations (A14) and (A15) are proved in Appendix B.

Equations (A14) and (A15), together with the definition of $F[A(t)|B(t')]$, give the fluctuation-dissipation theorem

$$\langle A(t)B(t')\rangle = \frac{1}{\beta}\int_{-\infty}^{\infty} d\omega\frac{\Lambda_{A,B}(\omega)}{\omega}e^{-i\omega(t-t')} + \langle A_0 B_0\rangle.$$
(A16)

Equation (21) in the main text is proved by taking $t = t'$ in the above equation.

APPENDIX B: PROOF OF THE STATIC CONTRIBUTION $C_{A,B} = 2\pi \langle A_0 B_0 \rangle$

In this Appendix, we discuss the properties of the zero-frequency component X_0 of an arbitrary variable X in general, and we prove Eqs. (A14) and (A15).

We first show that for a general variable $X(q, p)$, there is a unique splitting $X(q, p) = X_0(q, p) + \tilde{X}(q, p)$, in which $X_0(q, p)$ is the zero-frequency component and $\tilde{X}(q, p)$ is the nonzero-frequency component. Writing $X[x(t), p(t)]$ at time t as $X(q, p; t)$ [$q = q(0)$ and $p = p(0)$], we can do a Fourier decomposition to it as

$$X(q, p; t) = X_0(q, p) + \sum_{n(\omega_n \neq 0)} X_n(q, p) e^{-i\omega_n t}. \quad \text{(B1)}$$

Here, $X_0(q, p)$ is the zero-frequency component of X, and the sum of other terms is the nonzero-frequency component. For a nonperiodic system, replace the sum by an integral and the following discussion still applies. Due to property (i) below, $X_0(q, p)$ is a conserved quantity and it can be written as $X_0(q, p) = X_0[q(t), p(t)]$. Hence the nonzero-frequency part $X[q(t), p(t)] - X_0[q(t), p(t)]$ is also a function of $q(t)$ and $p(t)$. This shows that for variable $X(q, p)$, we have a well-defined and unique splitting $X(q, p) = X_0(q, p) + \tilde{X}(q, p)$.

We have the following useful statements about X_0, $\tilde{X}$, and general conserved quantities:

(i) $\{X_0, H\} = 0$. This is easily obtained from $\partial X_0(q, p)/\partial t = 0 = \{X_0, H\}(q, p)$. It shows that the static component of any variable X is a conserved quantity.

(ii) $\langle \{X_0, O\} \rangle = 0$ for any variable O. This can be obtained from $\langle \{X_0, O\} \rangle = \beta \langle \{X_0, H\} O \rangle = 0$. Here property (i) is used. It follows from (ii) that X_0 is orthogonal to any dynamical variable O under the inner product Eq. (32). That is, $(X_0|O) = 0$. To show this, we substitute O in (ii) by $\{O^*, H\}$, take a complex conjugate, and assume that $H^* = H$. In particular, $(X_0|X_0) = 0$, meaning X_0 has zero length under the inner product Eq. (32).

(iii) The space of conserved variables is the space of zero length variables. On the one hand, a conserved variable A fulfills $\{A, H\} = 0$ by definition. We have $(A|A) = \langle \{A^*, \{A, H\}\} \rangle = 0$, i.e., A has zero length. On the other hand, if a variable A has zero length, i.e., $(A|A) = 0$, we have $0 = \langle \{A^*, \{A, H\}\} \rangle = \beta \langle \{A^*, H\} \{A, H\} \rangle$. This implies $\{A, H\} = 0$. Mathematically, this space is called the null space of the Liouville operator, $\mathcal{L} = \{\ldots, H\}$.

(iv) $\langle A_0 \tilde{B} \rangle = \langle \tilde{A} B_0 \rangle = 0$ for any two variables A and B.

From Eq. (B1), we can write $\langle A_0 \tilde{B} \rangle = \sum_{n(\omega_n \neq 0)} \langle A_0 B_n \rangle$, employing the time translational invariance of the equilibrium state. We also have $\partial \tilde{X}(q, p; t)/\partial t = \sum_{n(\omega_n \neq 0)} \{X_n(q, p), H\} e^{-i\omega_n t} = \sum_{n(\omega_n \neq 0)} (-i\omega_n) X_n(q, p) e^{-i\omega_n t}$. It gives $\{X_n(q, p), H\} = -i\omega_n X_n(q, p)$. Applying it to B_n, we have $\langle A_0 \tilde{B} \rangle = \sum_{n(\omega_n \neq 0)} (-1/i\omega_n) \langle A_0 \{B_n, H\} \rangle = \sum_{n(\omega_n \neq 0)} (1/i\omega_n) \langle \{A_0, H\} B_n \rangle = 0$. Similarly, $\langle \tilde{A} B_0 \rangle = 0$. In particular, letting $B = c \neq 0$ be a constant, we obtain $\langle \tilde{A} \rangle = 0$ for arbitrary variable A.

Having obtained these properties, we consider the relaxation function $F[A(t)|B(t')]$ defined in Eq. (A2). Now we have $F[A(t)|B(t')] = \langle [A_0 + \tilde{A}(t)][B_0 + \tilde{B}(t')] \rangle$. Using (iv) and doing Fourier transformation, we obtain

$$F(A|B)_\omega = F(\tilde{A}|\tilde{B})_\omega + 2\pi \langle A_0 B_0 \rangle \delta(\omega). \quad \text{(B2)}$$

Equation (A11) gives

$$F(\tilde{A}|\tilde{B})_\omega = \frac{2\pi}{\beta \omega} \Lambda_{\tilde{A}, \tilde{B}}(\omega). \quad \text{(B3)}$$

From the definitions of retarded Green's function $G^r[A(t)|B(t')]$ in Eq. (5) and the spectral function $\Lambda_{A,B}(\omega)$ in Eq. (22), using (ii), we can easily confirm that both depend only on the nonzero-frequency components of A and B. That is, $G(A|B)_\omega = G(\tilde{A}|\tilde{B})_\omega$ and $\Lambda_{A,B}(\omega) = \Lambda_{\tilde{A}, \tilde{B}}(\omega)$. Putting the latter equation into Eqs. (B2) and (B3), we obtain

$$F(A|B)_\omega = \frac{2\pi}{\beta \omega} \Lambda_{A,B}(\omega) + 2\pi \langle A_0 B_0 \rangle \delta(\omega). \quad \text{(B4)}$$

This completes the proof of Eqs. (A14) and (A15).

[1] J. O. Hirschfelder, C. F. Curtiss, and R. B. Bird, *Molecular Theory of Gases and Liquids* (Wiley, New York, 1954).

[2] P. G. Debenedetti and F. H. Stillinger, Nature (London) **410**, 259 (2001).

[3] S. Lepri, R. Livi, and A. Politi, Phys. Rep. **377**, 1 (2003).

[4] M. Fujimoto, *The Physics of Structural Phase Transitions*, 2nd ed. (Springer, New York, 2005).

[5] S. P. Das, Rev. Mod. Phys. **76**, 785 (2004).

[6] T. Yokota, J. Haruyama, and O. Sugino, Phys. Rev. E **104**, 014124 (2021).

[7] T. Dauxois, M. Peyrard, and A. R. Bishop, Phys. Rev. E **47**, 684 (1993).

[8] B. Loubet, M. Manghi, and J. Palmeri, J. Chem. Phys. **145**, 044107 (2016).

[9] P. C. Martin and J. Schwinger, Phys. Rev. **115**, 1342 (1959).

[10] N. N. Bogoliubov and S. V. Tyablikov, Dokl. Akad. Nauk SSSR **126**, 53 (1959).

[11] S. V. Tyablikov, Ukr. Mat. Zh. **11**, 287 (1959).

[12] D. N. Zubarev, Usp. Fiz. Nauk **71**, 71 (1960) [Sov. Phys. Usp. **3**, 320 (1960)].

[13] N. N. Bogoliubov and B. I. Sadovnikov, Zh. Eksp. Theor. Fiz. **43**, 677 (1962) [Sov. Phys. JETP **16**, 482 (1963)].

[14] J. C. Herzel, J. Math. Phys. **8**, 1650 (1967).

[15] N. Rostoker, Nucl. Fusion **1**, 101 (1961).

[16] R. Aronson, J. Math. Phys. **7**, 589 (1966).

[17] J. C. Herzel, Phys. Lett. A **27**, 654 (1968).

[18] J. C. Herzel, J. Math. Phys. **11**, 741 (1970).

[19] T. Tanaka, K. Moorjani, and T. Morita, Phys. Rev. **155**, 388 (1967).

[20] M. J. Smith, Phys. Rev. Lett. **24**, 1398 (1970).

[21] L. S. Campana, A. Caramico D'Auria, M. D'Ambrosio, U. Esposito, L. De Cesare, and G. Kamieniarz, Phys. Rev. B **30**, 2769 (1984).

[22] O. K. Kalashnikov and E. S. Fradkin, Phys. Status Solidi B **59**, 9 (1973).

[23] A. Cavallo, F. Cosenza, and L. De Cesare, Phys. Rev. B **66**, 174439 (2002).

[24] For a review, see A. Cavallo, F. Cosenza, and L. De Cesare, in *New Developments in Ferromagnetism Research*, edited by V. N. Murray (Nova Science, New York, 2005), Chap. 6.

[25] A. Cavallo, F. Cosenza, and L. De Cesare, Phys. Rev. Lett. **87**, 240602 (2001).

[26] L. S. Campana *et al.*, Physica A **391**, 1087 (2012).

[27] L. S. Campana *et al.*, Physica A **471**, 629 (2017).

[28] For examples of recent research activities with this method, see Y. L. Liu, Int. J. Mod. Phys. B **32**, 1850258 (2018); **33**, 1950355 (2019); **35**, 2150064 (2021).

[29] H. Mori, Prog. Theor. Phys. **33**, 423 (1965); **34**, 399 (1965).

[30] R. Zwanzig, *Nonequilibrium Statistical Mechanics* (Oxford University Press, New York, 2001).

[31] P. Fan, K. Yang, K. H. Ma, and N. H. Tong, Phys. Rev. B **97**, 165140 (2018).

[32] K. Aoki and D. Kusnezov, Phys. Lett. A **265**, 250 (2000); Phys. Lett. B **477**, 348 (2000).

[33] B. Hu, B. Li, and H. Zhao, Phys. Rev. E **61**, 3828 (2000).

[34] K. Aoki and D. Kusnezov, Phys. Rev. E **68**, 056204 (2003).

[35] K. Aoki, J. Lukkarinen, and H. Spohn, J. Stat. Phys. **124**, 1105 (2006).

[36] A. Dhar, Adv. Phys. **57**, 457 (2008).

[37] N. Li and B. Li, Phys. Rev. E **76**, 011108 (2007); **87**, 042125 (2013).

[38] L. Xu and L. Wang, Phys. Rev. E **94**, 030101(R) (2016); **95**, 042138 (2017).

[39] N. Li, J. Liu, C. Wu, and B. Li, New J. Phys. **20**, 023006 (2018).

[40] W. G. Hoover and K. Aoki, Commun. Nonlin. Sci. Numer. Simulat. **49**, 192 (2017).

[41] K. Aoki, Comput. Methods Sci. Technol. **24**, 83 (2018).

[42] J. Liu, B. Li, and C. Wu, Europhys. Lett. **114**, 40002 (2016).

[43] N. Li, P. Tong, and B. Li, Europhys. Lett. **75**, 49 (2006).

[44] S. Liu, J. Liu, P. Hänggi, C. Wu, and B. Li, Phys. Rev. B **90**, 174304 (2014).

[45] H. Goldstein, C. P. Poole, and J. L. Safko, *Classical Mechanics*, 3rd edition (Pearson Education, London, 2002), Chap. 9.

[46] B. Jönsson, C. Peterson, and B. Söderberg, J. Phys. Chem. **99**, 1251 (1995).

[47] K. W. H. Stevens and G. A. Toombs, Proc. Phys. Soc. **85**, 1307 (1965).

[48] J. G. Ramos and A. A. Gomes, IL Nuovo Cimento A **3**, 441 (1971).

[49] P. Fröbrich and P. J. Kuntz, Phys. Rev. B **68**, 014410 (2003).

[50] P. Fröbrich and P. J. Kuntz, J. Phys.: Condens. Matter **17**, 1167 (2005).

[51] P. Fan and N. H. Tong, Chin. Phys. B **28**, 047102 (2019).

[52] K. H. Ma and N. H. Tong, Phys. Rev. B **104**, 155116 (2021).

[53] I. Pregogine, *Nonequilibrium Statistical Thermodynamics* (Consultants Bureau, New York, 1974).

[54] D. Boyanovsky, C. Destri, and H. J. de Vega, Phys. Rev. D **69**, 045003 (2004).

[55] K. Aoki and D. Kusnezov, Phys. Rev. Lett. **86**, 4029 (2001).

[56] Y. Onodera, Prog. Theor. Phys. **44**, 1477 (1970).

[57] K. H. Ma and N. H. Tong (unpublished).

[58] Y. V. Lvov and M. Onorato, Phys. Rev. Lett. **120**, 144301 (2018).

[59] M. Pettini and M. Landolfi, Phys. Rev. A **41**, 768 (1990).

[60] M. Pettini and M. Cerruti-Sola, Phys. Rev. A **44**, 975 (1991).

[61] D. He, S. Buyukdagli, and B. Hu, Phys. Rev. E **78**, 061103 (2008).

[62] For example, S. Aubry, J. Chem. Phys. **62**, 3217 (1975); **64**, 3392 (1976).

[63] D. Chen, S. Aubry, and G. P. Tsironis, Phys. Rev. Lett. **77**, 4776 (1996).

[64] K. Aoki and D. Kusnezov, Ann. Phys. **295**, 50 (2002).

[65] N. Li, J. Ren, L. Wang, G. Zhang, P. Hänggi, and B. Li, Rev. Mod. Phys. **84**, 1045 (2012).

[66] K. Niss and T. Hecksher, J. Chem. Phys. **149**, 230901 (2018).

[67] F. Arceri, F. P. Landes, L. Berthier, and G. Biroli, Glasses and Aging, in *A Statistical Mechanics Perspective*, edited by B. Chakraborty, Statistical and Nonlinear Physics, Encyclopedia of Complexity and Systems Science Series (Springer, New York, 2022).

[68] A. Naji, M. Kandu, J. Forsman, and R. Podgornik, J. Chem. Phys. **139**, 150901 (2013).

[69] M. H. Lee, Phys. Rev. B **26**, 2547 (1982).

[70] Yu. A. Tserkovnikov, Theor. Math. Phys. **49**, 993 (1981); **118**, 85 (1999); A. Belkasri and J. L. Richard, Phys. Rev. B **50**, 12896 (1994).